Design of Gram-Negative Selective Antimicrobial Peptides†

Steven A. Muhle and James P. Tam*

Department of Microbiology and Immunology, Vanderbilt University, A5119 MCN, Nashville, Tennessee 37232

Received January 5, 2001; Revised Manuscript Received March 7, 2001

ABSTRACT: Lipopolysaccharide (LPS), a major component of Gram-negative bacteria, signals bacterial invasion and triggers defensive host responses. However, excessive responses also lead to the serious pathophysiological consequence of septic shock. To develop Gram-negative selective compounds that can inhibit the effects of LPS-induced sepsis, we have designed constrained cyclic antimicrobial peptides based on a cystine-stabilized β-stranded framework mimicking the putative LPS-binding sites of the LPS-binding protein family. Our prototype termed R4A, c(PAC**R**C**R**AG-PA**R**C**R**CAG), consists of an eight amino acid degenerated repeat constrained by a head-to-tail cyclic peptide backbone and two cross-bracing disulfides. NMR study of K4A, an R4A analogue with four Arg → Lys replacements, confirmed the amphipathic design elements with four Lys on one face of the antiparallel β-strand and two hydrophobic cystine pairs plus two Ala on the opposite face. K4A and R4A displayed moderate microbicidal potency and Gram-negative selectivity. However, R4A analogues with single or multiple replacements of Ala and Gly with Arg or bulky hydrophobic amino acids displayed increased potency and selectivity in both low- and high-salt conditions. Analogues R5L and R6Y containing additional cationic and bulky hydrophobic amino acids proved the best mimics of the amphipathic topology of the "active-site" β-strands of LPS-binding proteins. They displayed potent activity against Gram-negative *E. coli* with a minimal inhibitory concentration of 20 nM and a >200-fold selectivity over Gram-positive *S. aureus*. Our results suggest that an LPS-targeted design may present an effective approach for preparing selective peptide antibiotics.

Gram-negative bacterial lipopolysaccharides (LPSs)[1] are well-known endotoxins with diverse structures that are displayed on bacterial outer membranes. They contain the conserved toxic moiety of lipid A, a fatty-acid-acylated and phosphorylated disaccharide (*1*−*3*). As a group, LPSs are one of the most potent bacterial signal molecules that activate host defenses to release proinflammatory mediators, cytokines, chemokines, and lipoproteins (*4*−*6*). However, when there are dysfunctional LPS-induced host inflammatory responses, release of tissue-damaging levels of cytokines and clotting-promoting tissue factors can lead to the pathophysiological consequence of septic shock. This major cause of morbidity and mortality has been estimated to cause over 100 000 deaths annually in the United States (*6*). Moreover, antibiotics currently used for Gram-negative infections result in the release of LPS into the bloodstream and thus cannot adequately treat sepsis.

Mechanisms that regulate host responses to LPS are known to involve plasma lipoproteins and the LPS-binding receptor CD14. These include the lipopolysaccharide-binding protein (LBP), bactericidal/permeability-increasing protein (BPI), phospholipid transfer protein (PLTP), serum amyloid P component (SAP), and antimicrobial proteins secreted by neutrophils (*7*−*12*). However, their binding to LPSs causes different cellular effects. Of these, the roles of LBP and BPI are best understood.

LBP is a lipid transfer protein whose facilitation of LPS binding to CD14 on cell membranes or soluble CD14 in plasma activates a wide variety of cells through Toll-like receptors (*13*−*15*). Circulatory LBP and CD14 may represent the major pathway for triggering host responses to the presence of LPS in the bloodstream and for mounting appropriate responses to Gram-negative bacteria. In contrast to the stimulatory properties of LBP, LPS binding by BPI is thought to be inhibitory, which accounts for its antibiotic activity against Gram-negative bacteria (*16*, *17*). Similar LPS-binding proteins have also been found in lower animals. Limulus anti-LPS factor (LALF) found in horseshoe crabs displays not only a strong affinity to LPS, but also selective

† This work was supported in part by NIH Grant CA36544 and by NIH Training Grant Fellowships 5T32GM07347 (S.A.M.) and 5T32CA09582.

* To whom correspondence should be addressed at the Department of Microbiology and Immunology, Vanderbilt University, A-5119 MCN, 1161 21st Ave. S., Nashville, TN 37232-2363. Telephone: (615) 343-1465, Fax: (615) 343-1467, E-mail: tamjp@ctrvax.vanderbilt.edu.

[1] Abbreviations: Amino acids and nomenclature of peptide structure are in accordance with the recommendations of the IUPAC−IUB (*53*). Other abbreviations are as follows: Acm, acetamidomethyl; BOP, benzotriazol-l-yloxytris(dimethylamino)phosphonium hexafluorophosphate; $C_2\beta2$, dicystine antiparallel β-stranded; $CC_2\beta2$, cyclic dicystine antiparallel β-stranded; $CC_3\beta2$, cyclic tricystine antiparallel β-stranded; CD, circular dichroism; CHCA, α-cyano-4-hydroxycinnamic acid; DCC, *N*,*N*-dicyclohexylcarbodiimide; DCM, dichloromethane; DIC, *N*,*N*-diisopropylcarbodiimide; DIEA, *N*,*N*-diisopropylethylamine; DMF, dimethylformamide; DMSO, dimethyl sulfoxide; DQF-COSY, double quantum filtered correlation spectroscopy; HF, hydrofluoric acid; HOBt, *N*-hydroxybenzotriazole; LPS, lipopolysaccharide; MALDI/MS, matrix-assisted laser desorption ionization mass spectrometry; MBHA resin, methylbenzhydrylamine resin; MIC, minimal inhibitory concentration; NMP, 1-methyl-2-pyrrolidinone; NOESY, nuclear Overhauser effect spectroscopy; RP-HPLC, reverse-phase high-performance liquid chromatography; TCEP, tris(carboxyethyl)phosphine; TFA, trifluoroacetic acid; TOCSY, total correlated spectroscopy; TSB, trypticase soy broth; SPPS, solid-phase peptide synthesis.

10.1021/bi0100384 CCC: $20.00
Published on Web 04/19/2001

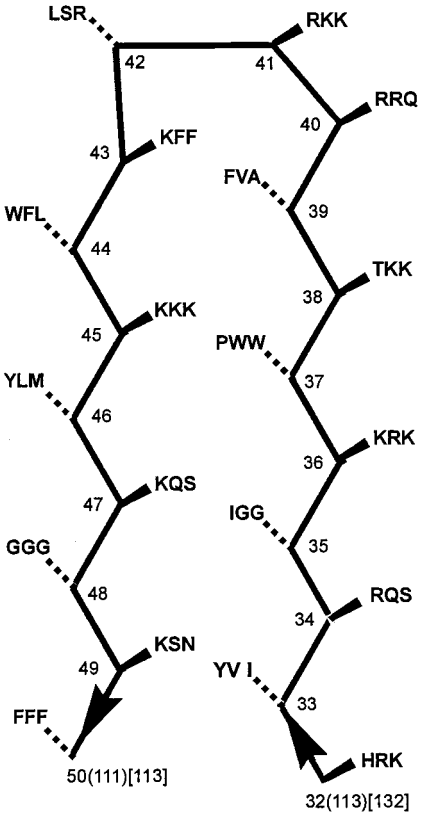

FIGURE 1: Amino acid sequences (from right to left) of the putative LPS-binding β-strands of Limulus anti-LPS factor (LALF, residues 32−50), LPS-binding protein (LBP, residues 111−130), and bactericidal permeability-increasing protein (BPI, residues 113−132).

antimicrobial activity against Gram-negative bacteria. Despite differences in their modes of action, the LPS-binding domains of LBP, BPI, and LALF have been found to share an interchangeable LPS-binding motif that is functionally independent of LPS transport or neutralization (*18*).

Cationic antimicrobial peptides with diverse structures have been reported to bind LPSs and thus suppress their ability to stimulate the production of proinflammatory cytokines (*19*−*23*). Recently, Scott et al. reported good correlation between the Gram-negative activity of certain antimicrobial peptides and their ability to block the interaction of LPS with LBP (*22*). Since antimicrobial peptides are generally low molecular mass molecules (<5 kDa) possessing broad-spectrum activities and constituting an important part of the host defense against microbial infections (*24*−*27*), they provide a starting point for designing low molecular mass anti-LPS compounds. Furthermore, they are known to have a propensity to fold into amphipathic structures with clusters of hydrophobic and charge regions, a feature closely related to their membranolytic activity. Because LPSs are also amphipathic molecules, LPS-binding antimicrobial peptides can neutralize LPS-induced toxicity and thus are potentially useful for treatment of septic shock and to temper aggressive host proinflammatory responses to LPS.

Our design of Gram-negative selective antimicrobial peptides is based on the putative LPS-binding domains of LBP, BPI, and LALF (*28*−*31*) consisting of a conserved motif of long β-strands with alternating basic and bulky hydrophobic amino acids (Figure 1). The up-and-down arrangement of side chains in an antiparallel β-strand produces a topological amphipathic motif that pairs the basic amino acids on one face with the hydrophobic amino acids on the opposite face. To provide the structural integrity of such a topological motif in our design, we use a cyclic dicystine-stabilized antiparallel β-stranded ($CC_2\beta2$) framework (*32*−*34*) modified from the Rhesus monkey theta defensin-1 (RTD-1). This recently discovered antimicrobial peptide with a $CC_3\beta2$ framework contains a cyclic tricystine antiparallel β-stranded structure (*35*). Our $CC_2\beta2$ structure also resembles the antimicrobial peptide family of the open-chain, dicystine-stabilized β-stranded ($C_2\beta2$) protegrins and tachyplesins (*36*, *37*) that consist of 17−19 amino acids (Figure 2). This paper describes the design, synthesis, and activities of a series of constrained $CC_2\beta2$ antimicrobial peptides with enhanced activity against Gram-negative bacteria. Two $CC_2\beta2$ prototypes, R4A and K4A (Figure 3), in our initial design displayed promising antimicrobial activity and selectivity. Incremental changes to R4A with the salient property of the putative LPS-binding β-strands markedly increased potency and selectivity against the test Gram-negative organism, *E. coli*. We have also determined the design elements of K4A by 2D NMR experiments and confirmed that four Lys are located on the hydrophilic face while there are two bracing disulfide pairs and two Ala on the opposite hydrophobic face.

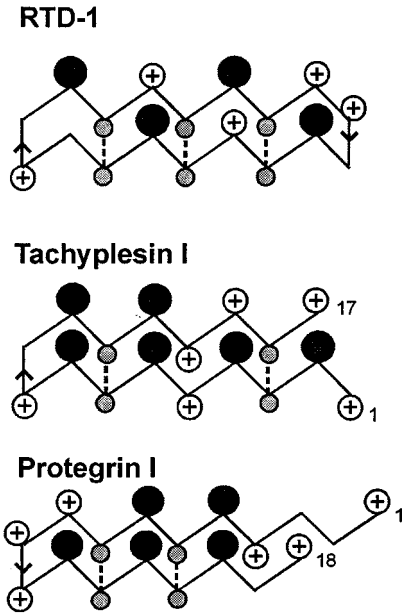

FIGURE 2: Amphipathic topology of RTD-1, TP-1, and PG-1. Pluses (+) indicate cationic residues, either Arg or Lys. Black circles indicate bulky hydrophobic residues: Leu, Val, Phe, Tyr, Trp. Gray circles connected by dashed lines indicate cystine pairs. Sequences are as follows: RTD-1, c(GFCRCLCRRGVCRCICTK); TP-1, KWCFRVCYRGICYRRCR; PG-1, RGGRLCYCRRRFCVCVGR.

MATERIALS AND METHODS

Materials. Boc-(*tert*-butyoxycarbonyl) amino acid derivatives and *N*-hydroxybenzotriazole (HOBt) were obtained from Chem-impex International Inc. All solvents, including acetonitrile (CH_3CN), dichloromethane (DCM), dimethylformamide (DMF), dimethyl sulfoxide (DMSO), and 1-methyl-2-pyrrolidinone (NMP) used without additional distillation, were obtained from EM Science. *N*,*N*′-Dicyclohexylcarbodiimide (DCC), *N*,*N*′-diisopropylethylamine (DIEA), α-cy-

Table 1: Sequence and Molecular Weights of $CC_2\beta 2$ Peptides[a]

peptide	residue 1	2	3	4	5	6	7	8	9	10	11	12	13	14	15	16	MW, calc/meas
R4A	P	A	C	R	C	R	A	G	P	A	R	C	R	C	A	G	1626/1626
K4A				K		K					K		K				1514/1514
R4Y										Y							1717/1717
R5Y								R		Y							1817/1817
R5W							W	R		Y							1932/1933
R5L		L					V	R		Y					V		1915/1915
R6A		R													R		1796/1796
R6F		R					Y			F					R	L	2020/2020
K5L		L		K		K	V	K		Y	K		K		V		1775/1776
E4A				E		E					E		E				1518/1518
E5L		L		E		E	V	E		Y	E		E		V		1779/1779

[a] Molecular weights were determined by MALDI mass spectrometry and rounded to the nearest whole number. The measured masses were all within 0.05% of the calculated mass.

ano-4-hydroxycinnamic acid, and *p*-cresol were purchased from Sigma−Aldrich Chemical Co. Trifluoroacetic acid (TFA) was obtained from Halocarbon. Tris(carboxyethyl)-phosphine (TCEP) came from Calbiochem. Ultrapure urea was obtained from ICN Biomedical and dialysis membrane from Spectrum Medical.

Test organisms obtained from the American Type Culture Collection (ATCC; Rockville, MD) were used for antimicrobial assays. These included Gram-negative *Escherichia coli* ATCC 25922, *Pseudomonas aeruginosa* ATCC 27853, and Gram-positive *Staphylococcus aureus* ATCC 29213 bacteria as well as *Candida albicans* ATCC 37092. The strains were incubated in trypticase soy broth (TSB), which was prepared in double-distilled water and autoclaved for sterilization. TSB was purchased from Becton−Dickinson (Cockeysville, MD).

Peptide Syntheses and Purification. Automated solid-phase peptide synthesis on an ABI 430A peptide synthesizer was performed using Boc-chemistry and a coupling protocol with DCC/HOBt in DMF/NMP (1:1, v/v). Analytical reverse-phase high-performance liquid chromatography (RP-HPLC) was conducted on a Shimadzu LG-6A system with a C_{18} Vydac column (4.6 × 250 mm) running a linear gradient of 10−90% buffer B for 30 min at 1 mL/min with detection at 225 mm. Eluent A: 0.04% TFA/H_2O; eluent B: 0.04% TFA/60% CH_3CN/H_2O. Preparative RP-HPLC was performed on a Waters 600 system with a C_{18} Vydac column (20 × 250 mm). Matrix-assisted laser desorption ionization mass spectrometry (MALDI-MS) was measured on a PerSeptive Biosystems Voyager instrument. Samples were dissolved in 1 μL of a 1:2 mixture of H_2O/CH_3CN. Measurements were made in a linear mode with α-cyano-4-hydroxycinnamic acid as the matrix.

Preparation of N-Terminal Cysteine Thioester Precursors. Precursors of cyclic peptides were assembled by Boc-chemistry solid-phase synthesis (*38*, *39*) on 0.26 mmol (1 g) of a detachable thiol resin, $HSCH_2CH_2CO$-MBHA resin (*40*, *41*). All four cysteines were uniformly protected with MeBzl. The assembled peptides were cleaved from the resin (250 mg) by high hydrofluoric acid (HF) treatment (HF/*p*-cresol/*p*-thiocresol, 9:1:0.1, v/v, 12 mL) for 75 min at 0 °C. After removal of HF by vacuum and washing with ether to remove the organic scavengers, the crude and deprotected peptides collected on a glass filter-funnel were extracted with 50 mL of 8 M urea, 0.2 M Tris, with 100 mg of TCEP (pH 5.6). Aliquots of crude unprotected peptide thioesters were purified to confirm their identity before cyclization.

Head-to-Tail Cyclization of N-Terminal Cysteinyl Thioester Peptide. Cyclization of the unprotected linear thioester precursors was performed as described by Tam et al. (*42*, *43*). Briefly, the extracted crude peptides in 8 M urea (50 mL) were dialyzed (MW cutoff 500) by sequentially lowering the urea concentration (2000 mL) from 8 M to 4 M and then 2 M urea, 0.2 M Tris buffered at pH 7.6 for 4 h each. The 12−18 h dialysis sequence also permitted concurrent cyclization that was monitored by analytical C_{18} RP-HPLC and MALDI-MS. In general, all cyclization reactions were complete by 18 h. For disulfide formation, the dialyzed peptide urea solution was further diluted with water to 1 M urea (300 mL), 10% DMSO was added, and disulfide bond formation was complete in 24 h as monitored by HPLC. MALDI-MS measurement determined the identity of these purified cyclic peptides and gave the expected values (Table 1).

NMR and CD Measurements. The 2D double quantum filtered correlation spectroscopy (DQF-COSY), total correlated spectroscopy (TOCSY), and nuclear Overhauser effect spectroscopy (NOESY) experiments (*44*) were performed under aqueous conditions on 500 MHz Bruker NMR equipment using Watergate graduated water suppression. Spin systems were identified on the TOCSY spectra, and proton assignments were made according to the sequential NOESY connectivities. The $^3J_{N,\alpha}$ vicinal couplings were measured from the DQF-COSY spectra. CD spectra were recorded on a Jasco J-720 spectropolarimeter over the wavelength range of 250−190 nm using a 1.0 mm path length cell, a bandwidth of 1.0 nm, a response time of 2 s, and averaging over three scans. The spectra are expressed as molar ellipticity, [θ].

Antimicrobial Assays. A two-stage radial diffusion antimicrobial assay described by Lehrer et al. (*46*) was employed. Antimicrobial activities were expressed in units (0.1 mm = 1 U) and the minimal inhibitory concentrations (MICs) determined from the *x*-intercepts of the dose−response curves. Two assay conditions were used: low salt that corresponds to typical bacterial media, and high salt (100 mM NaCl) that corresponds to serum salt conditions.

LPS Neutralization Assay. The ability of selected peptides to neutralize LPS was tested with the *Limulus* amoebocyte lysate assay (LAL) according to the manufacturer's instruc-

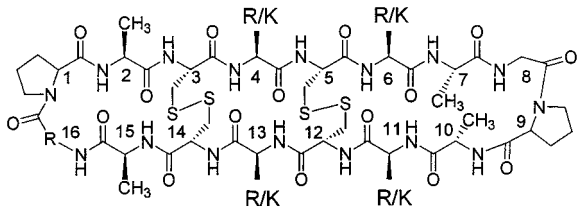

FIGURE 3: Schematic representation of the $CC_2\beta2$ design of R4A/K4A. Note: subsequent analogues are derived from R4A by substitutions at positions 2, 7, 8, 10, 15, or 16.

tions (Bio Whittaker) using *Escherichia coli* 055:B5 LPS. This assay is an extremely sensitive indicator of the presence of free, nonneutralized LPS, which activates the *Limulus* coagulation cascade leading to gelation of the lysate (*47*). LPS specific activity was determined by a serial dilution series to show the concentration required to activate the coagulation cascade. Three selected peptides, R4A, R5L, and R6F, and a positive control, polymyxin B (PMB), were assayed with a semilogarithmic dilution to reveal the minimal concentration for inhibition of LPS-induced gelation.

RESULTS AND DISCUSSION

Design of $CC_2\beta2$ Prototypes R4A and K4A. The $CC_2\beta2$ prototypes R4A and K4A (Figure 3) contain two degenerated octapeptide repeating sequences of five amino acids (Gly, Pro, Cys, Ala, and Arg/Lys) and a cyclic structure of c(PACXCXAG-PAXCXCAG) where X = R in R4A and X = K in K4A. Three of these amino acids are used for structural roles. Four of the Cys residues form two cross-bracing disulfides that can position a cationic cluster of four Lys or Arg at the top face, similar to the putative LPS-binding sites of LBP, BPI, and LALF with charged amino acids in the middle of a long β-strand. The Gly-Pro reverse turns form the two ends flanking a pair of Ala in two Ala-Gly-Pro-Ala sequences. These design elements were intended to generate a rigid pseudo-symmetric antiparallel β-strand scaffold with an amphipathic top−bottom face mimicking the LPS-binding loop of the LPS-binding protein family. The use of simple amino acids in R4A and K4A was also intended to facilitate structural determination of the peptides by NMR. These cyclic peptides consisting of 16 amino acids are slightly smaller than the open-chain, β-stranded protegrins and tachyplesins that range in length from 17 to 19 residues. K4A was designed to mimic the putative LPS-binding sites of LBP, BPI, and LALF that are rich in Lys, whereas R4A was designed to mimic the Arg-rich protegrins, tachyplesins, and RTD-1. Except for the four Arg → Lys replacements, the other design elements of R4A and K4A were similar.

Synthesis. The synthetic plan to prepare R4A, K4A, and other $CC_2\beta2$ peptides consisted of two reactions. An on-resin stepwise solid-phase synthesis by Boc-chemistry was used to prepare linear peptide precursors with an amino (N)-terminal Cys and a carboxyl (C)-terminal thioester. An off-resin thioester cyclization of the linear unprotected peptide thioesters produced the macrocyclic peptides. The C-terminal thioester was prepared from a *p*-methylbenzhydrylamine resin coupled to mercaptopropionic acid to give a removable thiopropionyl linker. Coupling of Boc-Ala, by DCC or BOP activation, formed the C-terminal Boc-Ala-thioester resin (*40*, *41*). Following assembly on a thioester resin and the removal of all protecting groups by HF, head-to-tail cyclization of the free peptide thioesters in aqueous conditions buffered at pH 7.6 afforded the macrocyclic peptides. Because of their circular permutated nature, any of the four Cys−Xaa bonds can be used as a starting point for the synthesis of the linear precursor to give the desired cyclic peptide. For example, the least hindered Cys−Ala bond in K4A was chosen as the site for the head-to-tail cyclization from the linear precursor thioester sequence of CKCKAGPAKCKCAGPA.

The cyclization rates to form K4A, R4A, and their corresponding analogues were found to be efficient and generally complete within 12 h. This efficiency is likely contributed by the multiple Cys in these 16-aa linear thioester precursors that facilitate lactamization under aqueous conditions by a thia-zip mechanism (*42*). The zip mechanism mediated by a series of thiol−thiolactone exchange reactions is initiated by one of the four cysteinyl thiols to form a thiolactone between the two termini of the linear K4A thioester under aqueous conditions at pH 7.6. Such an intramolecular transthioesterification is rapid, reversible, and proximity-driven that favors the formation of a small thiolactone. Since there are four thiols present in the K4A sequence, a series of thiol−thiolactone exchanges similar to a zip reaction leads ultimately to the formation of an N-terminal thiolactone through smaller thiolactone intermediates. Once the N-terminal thiolactone is formed, a spontaneous and irreversible ring contraction via an *S,N*-acyl shift affords the desired Cys−Ala bond. The resulting cyclic peptide was immediately oxidized with 10% DMSO in a buffered aqueous solution at pH 7.6 and purified by C_{18} RP-HPLC. According to MALDI-MS, the purified K4A had a molecular mass of 1514 Da, which is in agreement with the calculated molecular mass. No oligomerization or end-to-side-chain cyclized products were detected as monitored by HPLC and MALDI-MS analyses. Thus, our synthetic scheme for preparing rigid cyclic peptides is facile, efficient, and, more importantly, regiospecific. It offers a significant improvement over conventional methods of cyclization using protected peptide segments and enthalpic activation. The antiparallel β-sheet design, coupled with DMSO-mediated oxidation, also favored the desired cross-stranded parallel disulfide pairings. Of three possible disulfide isomers, only the desired disulfide isomer was detected throughout this series of 12 analogues.

1D and 2D NMR Characterization of Cyclic Peptide K4A. The positions of the disulfide bonds were determined by comparing a 1D spectrum of cyclic monocystine K4A, [Abu^{3,14}]K4A, with β-aminobutyric acid (Abu) substituting for Cys3 and -14 (data not shown). The αH chemical shifts for Cys5 and Cys12 (4.70, 4.63 ppm), common to K4A and [Abu^{3,14}]K4A, are identical in both peptides and provide firm assignment of the Cys3 and Cys14 disulfide bond in K4A. The secondary structural elements were determined by the 2D DQF-COSY, TOCSY, and NOESY experiments. The residue assignments and chemical shifts are shown in Table 2.

The dipolar connectivities obtained from the NOESY experiments (Figure 4) were used to determine secondary structural elements. Since $J_{\alpha N}$ coupling constants follow the Karplus equation, they are predicted to be about 9 Hz for the extended β-sheet. Values of $J_{\alpha N} > 8$ Hz are found in all

Table 2: Chemical Shifts of K4A in 5% D_2O/H_2O at 25 °C, pH 5.0

	NH	Hα	Hβ	Hγ	Hδ	Hε
P-1		4.32	2.20	1.92	3.51, 3.67	
A-2	8.38	4.32	1.29			
C-3	7.53	4.48	2.85, 2.96			
K-4	8.66	4.38	1.74	1.39	1.62	2.92
C-5	8.19	4.70	2.96, 3.04			
K-6	8.68	4.24	1.74	1.37	1.62	2.92
A-7	8.04	4.26	1.34			
G-8	7.93	3.83, 4.34				
P-9		4.32	2.20	1.92	3.51, 3.67	
A-10	8.08	4.22	1.32			
K-11	7.98	4.20	1.74	1.34	1.62	2.92
C-12	8.25	4.63	3.03, 3.08			
K-13	8.71	4.38	1.83	1.30	1.63	2.92
C-14	7.77	4.48	2.88, 3.21			
A-15	8.51	4.48	1.30			
G-16	8.28	4.36, 3.88				

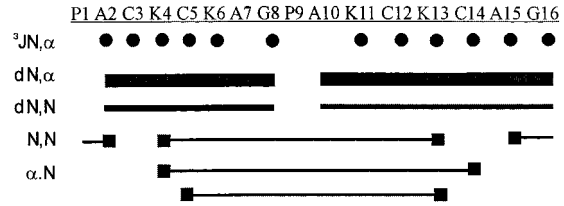

FIGURE 4: Nuclear Overhauser effect. $J_{N,\alpha}$ coupling >8 Hz is indicated by black circles. Strong short-range NOEs are indicated by thick black bars; long-range NOEs are indicated by connected black boxes.

four lysines (Lys4, -6, -11, and -13) and cysteines (Cys3, -5, -12, and -14), and in two alanines (Ala2 and Ala15), indicating a stable extended β-sheet conformation of Ala2 to Cys6 and Cys12 to Ala15. The presence of strong sequential and long-range NOE cross-peaks also suggests an antiparallel β-sheet structure. Ala7 and Ala10, both of which couple at 6.4 Hz, are suggestive of a bulge or bend at one end of the peptide. This may occur because the Gly-Pro at the Cys5→Cys12 turn is larger and, therefore, more flexible than the corresponding Gly-Pro Cys14→Cys3 turn. The strong $d_{N,\alpha}$ connectivities with weaker $d_{N,N}$ connectivities are also characteristic of an antiparallel β-sheet structure (*44*). This conformation is further supported by long-range NOEs between the amides of Ala2→Ala15, Cys3→Lys13, and the Hα/amide interaction between Cys14→Lys4, Cys5→Lys13. These residues must be in relatively close proximity to generate the NOE accounting for an antiparallel β-sheet conformation. The strong coupling of the glycine residues and the innate structural constraints of the proline suggest type II β-turns.

The data are consistent with the proposed structure consisting of a rigid antiparallel β-sheet. The identified structure places all four lysines in a unidirectional configuration shown in Figure 3. The addition of the two disulfide linkages also provides greater rigidity to the template that permits a well-defined structure of K4A to be determined in aqueous conditions.

Our series of $CC_2\beta2$ peptides were also characterized by circular dichroism (CD) spectroscopy in aqueous solutions (*45*). The CD spectra obtained were similar to the three series of $CC_2\beta2$ peptides of protegrins, tachyplesins, and RTD-1 previously reported by us (*32*−*34*). Such spectra are consistent with the presence of type II β-turns with an antiparallel β-sheet secondary structure. The peptides display characteristic red-shifted n−π* minima near 224 nm and strong π−π* minima between 192 and 197 nm (data not shown).

Antimicrobial Activity and Selectivity of K4A and R4A. A two-stage radial diffusion assay in agarose gels (*46*) was employed to test K4A, R4A, and their analogues against four organisms under both high-salt (with 100 mM NaCl) and low-salt (without NaCl) conditions. The former simulates physiological conditions and provides a useful guide to the therapeutic potential of an antimicrobial peptide. The antimicrobial activity of each peptide was expressed as the minimum inhibitory concentrations (MICs) of 0.01 to >500 μM (Table 3). We used the MIC ratios of two model organisms to indicate Gram-negative selectivity, Gram-positive *S. aureus*/Gram-negative *E. coli*.

K4A displayed a wide spectrum of activity against the four test organisms with MICs ranging from 4.8 to >500 μM under both low- and high-salt conditions. With the exception of *C. albicans*, the activity of K4A was abrogated against all organisms under high-salt conditions. Under low-salt conditions, R4A was the more active of these two prototypic peptides with MICs at 1−45 μM. Under high-salt conditions, R4A had no activity against *S. aureus* and *P. aeruginosa*,

Table 3: Antimicrobial Activity of $CC_2\beta2$ Peptides[a]

	MIC (μM)									
	S. aureus		*E. coli*		*P. aeruginosa*		*C. albicans*		Gram-negative selectivity[c]	
peptide	H[b]	L[b]	H	L	H	L	H	L	H	L
K4A	>500	40	>500	4.8	>500	>500	7.0	6.0	–	8.3
R4A	>500	45	19.0	1.0	>500	11.0	6.8	6.2	26	45
R4Y	>500	40	21.0	1.0	180	11.2	6.3	6.8	24	40
R5Y	50	10	2.05	0.2	1.8	1.8	1.3	1.4	25	50
R5W	>500	30	2.05	0.07	5.0	2.0	2.6	2.5	250	429
R5L	50	4.0	0.64	0.02	1.0	0.9	1.6	0.8	78	200
R6A	>500	30	17.0	0.18	17.0	2.8	3.0	2.2	29	167
R6F	50	5.0	0.24	0.02	2.1	0.3	1.3	1.0	208	250
K5L	>500	7.0	>500	5.0	>500	>500	ND[d]	ND[d]	–	1.4
E4A	>500	>500	>500	>500	>500	>500	>500	>500	–	–
E5L	>500	>500	>500	>500	>500	>500	>500	>500	–	–
TP-1	0.5	0.4	0.4	0.3	0.5	0.9	0.9	0.7	1.2	1.3
PG-1	0.6	0.7	0.8	0.9	2.0	1.2	1.0	1.3	0.75	0.78
RTD-1	0.9	1.1	28.4	2.0	5.2	2.0	5.2	4.0	0.03	0.55

[a] Antimicrobial activity was determined by radial diffusion assay and is expressed as minimal inhibitory concentration (MIC, μM). [b] H = high salt (100 mM NaCl), L = low salt. [c] Selectivity = MIC *S. aureus* (Gram-positive)/MIC *E. coli* (Gram-negative). [d] ND = not determined.

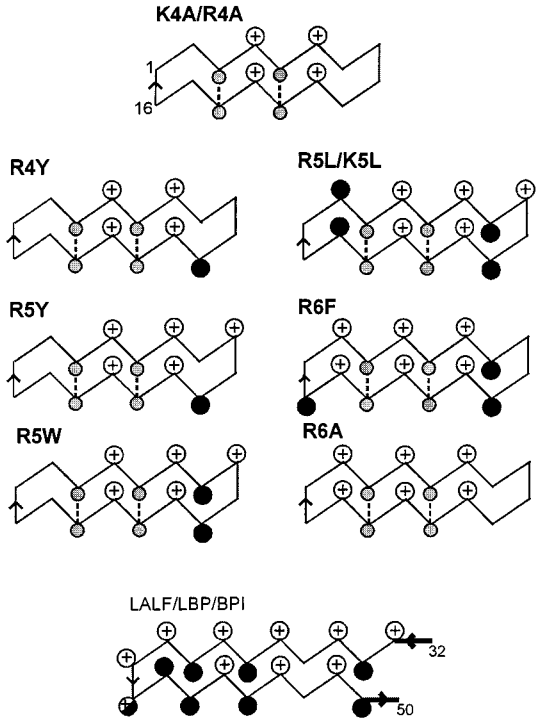

FIGURE 5: Amphipathic topology of $CC_2\beta2$ peptide series. Pluses indicate cationic residues, either Arg or Lys. Black circles indicate bulky hydrophobic residues: Leu, Val, Phe, Tyr, Trp (LBP/BPI also contains Met, Ile, His, Gln). Gray circles connected by dashed lines indicate cystine pairs. Sequences of R4A and its analogues, TP-1 as well as PG-1, are found in Table 1 and Figure 2.

but retained activity against *E. coli*. Furthermore, R4A and K4A displayed Gram-negative selectivities of 8- and 45-fold, respectively, under low-salt conditions (Table 3). It is also encouraging to note that R4A exhibited Gram-negative selectivity of >26-fold under high-salt conditions. These results suggest that Arg is more suitable than Lys as a cationic amino acid to improve the design of $CC_2\beta2$ peptides that can tolerate high-salt conditions and be selective for Gram-negative bacteria. Based on these results, R4A was used as a template for subsequent analogue refinements.

Refinements of R4A Analogues. As shown in Figure 5, the top faces of the putative LPS-binding β-strands are essentially cationic with >8 Lys and Arg whereas the bottom faces are hydrophobic with bulky hydrophobic amino acids consisting of Phe, Tyr, Trp, Leu, Ile, and Val. To better mimic the LPS-binding β-strands, one K4A and six R4A analogues (Table 1) with graded increases of cationic charges and bulky hydrophobic amino acids were prepared by substituting Ala or Gly at or near the reverse turns of the $CC_2\beta2$ scaffold (Figure 5). Peptides R4Y and R5Y contain one or two amino acid changes whereas peptide R5W contains three. Finally, the four or five substitutions in R5L, K5L, R6A, and R6Y make the numbers of their charged and hydrophobic residues comparable to those of the putative LPS-binding β-strand of LPS-binding proteins.

We first focused on mutating Ala7, Gly8, and Ala10 at the right half of the $CC_2\beta2$ R4A scaffold (Figure 3). The first analogue, R4Y with a single Ala10→Tyr substitution, had increased high-salt activity against *P. aeruginosa*, but other activities and selectivities were largely unchanged. Further modification of R4Y through the Gly8→Arg substitution in R5Y to give five Arg on the top face of the $CC_2\beta2$ scaffold resulted in a 5−100-fold increase in potency and improved the MIC against *E. coli* to 0.2 μM. More significantly, the addition of the positively charged Arg enabled R5Y to be salt-insensitive with MICs <2.1 μM against three test organisms and an MIC of 50 μM against *S. aureus*. Adding another bulky hydrophobic Trp residue to R5Y at the bottom face by the Ala7→Trp substitution in R5W resulted in a 3-fold decrease of Gram-positive potency against *S. aureus* concomitant with an increase to 70 nM in Gram-negative potency against *E. coli* in low-salt conditions. Interestingly, the Ala7→Trp substitution completely abrogated Gram-positive activity under high-salt conditions. R5W is the most selective of the three analogues with mutations of the $CC_2\beta2$ R4A scaffold. It displays Gram-negative selectivity of 429 and >250 under low- and high-salt conditions, respectively.

We then mutated residues Ala2, Ala15, and Gly16 at the left half of the $CC_2\beta2$ R4A scaffold (Figure 3). Building on the favorable results of Gly8→Arg replacement in R5Y, R5L was designed to retain the five Arg on the top face. In addition, all four Ala in R5Y were globally substituted by four bulky amino acids (Leu2, Val7, Tyr10, and Val15) to increase the hydrophobicity of the molecule. To provide a different cationic topology on the top face, peptide R6Y was designed to contain a cluster of six Arg in the middle of the molecule by substituting Arg for the two top-face Ala, Ala2 and Ala15. R6F also contained three bulky hydrophobic amino acids, two at the bottom face (Tyr7, Phe10) and one at the reverse turn (Leu16). Compared with R4A, the potency (MIC) and selectivity of R5L and R6F against *E. coli* in low-salt conditions were increased 50-fold to 20 nM and >200, respectively. Activity and selectivity in high-salt conditions also increased significantly, ranging from 0.64 μM and 78 for R5L to 0.24 μM and 208 for R6F, respectively. R6A, a highly positively charged peptide without the additional hydrophobic groups of R6F, had no increase in Gram-positive activity, but displayed a 5-fold increase of Gram-negative activity and selectivity under low-salt conditions.

To test the difference between Lys and Arg, K5L was prepared to contain five Arg→Lys replacements. The result of the Arg→Lys substitutions in K5L was a significant loss of potency and selectivity. Under low-salt conditions, K5L with an MIC of 5 μM was 250-fold less active than R5L against *E. coli* and was inactive against *P. aeruginosa*, but its potency was similar to R5L against *S. aureus*. Furthermore, K5L with Arg→Lys substitutions lost all activity against all three bacteria in high-salt conditions. Together with the results observed in the peptides K4A and R4A, Arg appears to be a more suitable cationic amino acid than Lys in the design of small and constrained β-stranded antimicrobial peptides with enhanced selectivity against *E. coli* and the ability to retain potency under high-salt conditions. To show that the cationic amino acids are essential for antimicrobial activity, we also prepared two acidic analogues, E4A and E5L, containing global Glu6Arg substitutions of R4A and R5L, respectively. Both acidic analogues were inactive.

Microbicidal activity against the yeast *C. albicans* varied little throughout the series, remaining in the 1−7 μM range. Microbicidal activity against the Gram-positive *S. aureus* in low-salt conditions varied only moderately, increasing from 45 to 5 μM from the least to the most potent, but their activity

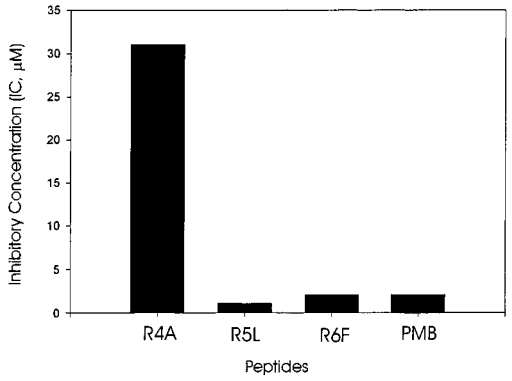

FIGURE 6: Inhibition of LPS-induced gelation by peptides in LAL assay. The inhibitory concentration (IC, μM) is the lowest concentration of peptide that inhibits LPS from inducing the LAL coagulation cascade. Polymixin B is used as the positive control.

is often abrogated in high-salt conditions. In contrast, the variability of the Gram-negative activity in low-salt conditions is high, with MICs against *E. coli* ranging from 0.018 to 5 μM and MICs against *P. aeruginosa* from 0.3 to >500 μM. Our results also show that the $CC_2\beta2$ peptides are selective for two test Gram-negative bacteria and generally display higher potency against *E. coli* than *P. aeruginosa*.

A minimum number of cationic and hydrophobic residues appear to be necessary for achieving Gram-negative selectivity in the $CC_2\beta2$ peptide series. The two potent peptides R5L and R6F contain a highly charged face with five or six Arg residues as well as a very hydrophobic face with three or four bulky hydrophobic groups in addition to two cystine bridges. Their activity profiles are relatively similar. They are both active against Gram-negative *E. coli* with MICs <0.7 μM in low-salt conditions and a >20-fold increase to 20 nM under low-salt conditions. In comparison, they are only moderately active against Gram-positive *S. aureus* in the 4−5 μM range. Furthermore, these two peptides are approximately 250 times more potent against *E. coli* than *S. aureus*. These results suggest that although broad-spectrum activity is present against all test organisms, the peptides R5L and R6F have selective activity against Gram-negative bacteria.

LPS-Binding Activity. To determine whether our designed peptides would bind to LPS and that the affinity for LPS binding would correlate with the antimicrobial activity against Gram-negative organisms, we examined the ability of three of the peptides to inhibit activation of the Limulus coagulation cascade by LPS (*47*). R4A, which had moderate activity against Gram-negative organisms, was able to inhibit gelation of the LAL assay in concentrations above 30 μM (Figure 6). The peptides R5L and R6F, which displayed significantly enhanced Gram-negative activity, were able to inhibit gelation at concentrations as low as 1 μM, which was comparable to inhibition by polymyxin B, a known potent inhibitor of LPS. Although each of the peptides tested in the LAL assay could inhibit LPS induction of the Limulus coagulation cascade, R4A was 30-fold less effective than both R5L and R6F in this assay. These results are consistent with the observation that R5L and R6F are, by comparison, about 50 times more active than R4A in the antimicrobial assay.

Comparison with Protegrins, Tachyplesins, and RTD-1. Our series of $CC_2\beta2$ peptides shares structural similarities to protegrins, tachyplesins, and RTD-1. Protegrins and tachyplesins are among the most potent broad-spectrum β-stranded antimicrobial peptides known to date. These peptides are highly amphipathic with many basic and bulky amino acids. Both protegrin-1 (PG-1) and tachyplesin-1 (TP-1) contain six basic amino acids that are either exclusively or predominantly Arg. PG-1 contains five bulky amino acids, of which two are aromatic (Phe and Tyr) and three are aliphatic (Leu and two Val) whereas TP-1 contains six: four aromatic (Trp, Phe, and two Tyr) and two aliphatic (Val, Ile). There are two cross-bracing disulfides on one face of the β-stranded structures that constitute the hydrophobic face of these peptides (Figure 5), which are equally active against both Gram-negative and Gram-positive bacteria with a Gram-negative selectivity ratio of about 1 under high-salt conditions (Table 3). Since we have prepared $CC_2\beta2$ analogues of protegrins, tachyplesins, and RTD-1 that retain activity spectra and potency similar to their native molecules (*32*−*34*), we can compare the structure−activity relationships of these three series of $CC_2\beta2$ peptides with R5L and R6F.

From a minimalist perspective, the $CC_2\beta2$ and the more rigid $CC_3\beta2$ scaffolds approximate a "β-tile"- or "β-tape"-like structure. The up-and-down side-chain arrangements on these rigid two-β-strand frameworks produce a top face containing clusters of hydrophobic and positively charged amino acids and a sulfur-rich hydrophobic bottom face formed by two cystine pairs. Because their structural rigidity is due to the β-tile-type arrangement, we can correlate their activity with the topology of the cationic and hydrophobic clusters. The amphipathic topologies of the Gram-negative selective R5L and R6F are characterized by a cationic top face and a hydrophobic bottom face. Such topology can be described as unipolar, with five or more cationic charged amino acids clustered on the top face of the $CC_2\beta2$ scaffold and hydrophobic amino acids at the bottom face, and bears a similarity to the LPS-binding β-strands of the LPS-binding proteins (Figure 5). In contrast, the amphipathic topology of protegrin-1 and tachyplesin-1, which are nonselective to both Gram-positive and Gram-negative bacteria, can be characterized as end-to-end bipolar with a cluster of four or more bulky hydrophobic amino acids in the middle of the molecule whereas the cationic charges are clustered at or near the end of the antiparallel β-strands (Figure 2). RTD-1, which is more selective for Gram-positive than Gram-negative bacteria, displays a slanting amphipathic topology with alternating clusters of cationic and hydrophobic amino acids. Thus, the topology of the charge and hydrophobic clusters may provide a useful guide to the design of selective peptide antibiotics using the $CC_2\beta2$ scaffolds.

CONCLUSIONS AND PERSPECTIVES

To address the current need for developing novel compounds to neutralize the effects of LPS-induced sepsis, we have designed highly constrained $CC_2\beta2$ antimicrobial peptides selective for Gram-negative bacteria by mimicking the alternating charge and hydrophobic motifs of the putative LPS-binding β-strands of the LPS-binding proteins. The structural design of the $CC_2\beta2$ prototypic K4A is confirmed by 2D NMR to contain an antiparallel β-sheet backbone. Two of our peptides, R5L and R6F, best mimic the up−down topology of LPS-binding β-strands with alternating charge and bulky hydrophobic amino acids, displaying MICs

of 20 nM against the Gram-negative *E. coli* and a selectivity of >200-fold over the Gram-positive *S. aureus.* Although BPI, a promising LPS-binding protein of 60 kDa, has an MIC of <1 nM against Gram-negative bacteria such as *E. coli*, it has a molecular mass 30-fold higher than R5L or R6F. Thus, it is encouraging to note that on a mass basis, R5L or R6F with a molecular mass of 2 kDa and an MIC of 20 nM approaches the activity of BPI, but has the advantage of being much smaller.

The small $CC_2\beta2$ antimicrobial peptides also provide an attractive template for structure−function study because of their conformational rigidity derived from a close-chain, two-β-stranded structure with two cross-braced disulfide bonds. Furthermore, cyclic peptides are likely to have more proteolytic resistance and often retain antimicrobial activity under physiological conditions of 100−150 mM NaCl (high-salt conditions) necessary for therapeutic applications (*24*−*27*, *32*−*37*).

There are precedents for naturally occurring, organism- or target-selective antimicrobial peptides. Breukink et al. (*48*) have reported that the antimicrobial peptide nisin Z is specific for the membrane-anchored cell-wall precursor Lipid II, which is also the target of the conventional antibiotic vancomycin. However, nisin Z binds to Lipid II with high affinity, rendering the plasma membrane more permeable. Similarly, the proposed killing mechanisms of proline-rich antimicrobial peptides such as apidaecin, drosocin, and pyrrhocoricin have been suggested to be intracellular bacterial proteins after their translocation inside bacteria (*49*, *50*). Our laboratory has shown that kalata (*51*), a plant-derived macrocyclic peptide containing a cystine-knot motif, is specific for the Gram-positive *S. aureus* with an MIC of 0.26 μM (*52*). It is essentially inactive against Gram-negative bacteria with an MIC >500 μM for *E. coli* and *P. aeruginosa*. RTD-1, a novel cyclic defensin-like peptide isolated from Rhesus macaque (*35*), is shown to be more selective for Gram-positive than Gram-negative bacteria (*32*). However, the molecular targets of kalata and RTD-1 have not been determined. These modes of action targeting specific proteins by antimicrobial peptides, in addition to their membranolytic activity, may provide a rational approach for developing new peptide antibiotics selective for targeting specific extracellular or intracellular microbial components.

ACKNOWLEDGMENT

We thank Drs. Yi-An Lu, Jin-Long Yang, and Andrej Krezel for their advice and technical assistance.

REFERENCES

1. Gallay, P., Heumann, D., Le Roy, D., Barras, C., and Glauser, M. P. (1993) *Proc. Natl. Acad. Sci. U.S.A. 90*, 9935−9938.
2. Gallay, P., Heumann, D., Le Roy, D., Barras, C., and Glauser, M. P. (1994) *Proc. Natl. Acad. Sci. U.S.A. 91*, 7922−7926.
3. Le Roy, D., Di Padova, F., Tees, R., Lengacher, S., Landmann, R., Glauser, M. P., Calandra, T., and Heumann, D. (1999) *J. Immunol. 162*, 7454−7460.
4. Ulevitch, R. J., and Tobias, P. S. (1995) *Annu. Rev. Immunol. 13*, 437−457.
5. Ingalls, R. R., Monks, B. G., Savedra, R., Jr., Christ, W. J., Delude, R. L., Medvedev, A. E., Espevik, T., and Golenbock, D. T (1998) *J. Immunol. 161*, 5413−5420.
6. Malhotra, R., and Bird, M. I. (1997) *Bioessays 19*, 919−923.
7. Schumann, R. R., Leong, S. R., Flaggs, G. W., Gray, P. W., Wright, S. D., Mathison, J. C., Tobias, P. S., and Ulevitch, R. (1990) *Science 249*, 1429−1431.
8. Wright, S. D., Ramos, R. A., Tobias, P. S., Ulevitch, R. J., and Mathison, J. C. (1990) *Science 249*, 1431−1433.
9. Tobias, P. S., Soldau, K., Gegner, J. A., Mintz, D., and Ulevitch, R. J. (1995) *J. Biol. Chem. 270*, 10482−10488.
10. Tobias, P. S., Mathison, J. C., and Ulevitch, R. J. (1988) *J. Biol. Chem. 263*, 13479−13481.
11. Elass-Rochard, E., Legrand, D., Salmon, V., Roseanu, A., Trif, M., Tobias, P. S., Mazurier, J., and Spik, G. (1998) *Infect. Immun. 66*, 486−491.
12. de Haas, C. J., van der Tol, M. E., Van Kessel, K. P., Verhoef, J., and Van Strijp, J. A. (1998) *J. Immunol. 161*, 3607−3615.
13. Yang, R. B., Mark, M. R., Gray, A., Huang, A., Xie, M. H., Zhang, M., Goddard, A., Wood, W. I., Gurney, A. L., and Godowski, P. J. (1998) *Nature 395*, 284−288.
14. Yang, R. B., Mark, M. R., Gurney, A. L., and Godowski, P. J. (1999) *J. Immunol. 163*, 639−643.
15. Schroder, N. W., Opitz, B., Lamping, N., Michelsen, K. S., Zahringer, U., Gobel, U. B., and Schumann, R. R. (2000) *J. Immunol. 165*, 2683−2693.
16. Tobias, P. S., Soldau, K., Iovine, N. M., Elsbach, P., and Weiss, J. (1997) *J. Biol. Chem. 272*, 18682−18685.
17. Dentener, M. A., Von Asmuth, E. J., Francot, G. J., Marra, M. N., and Buurman, W. A. (1993) *J. Immunol. 151*, 4258−4265.
18. Schumann, R. R., Lamping, N., and Hoess, A. (1997) *J. Immunol. 159*, 5599−5605.
19. Gough, M., Hancock, R. E., and Kelly, N. M. (1996) *Infect. Immun. 64*, 2005.
20. Larrick, J. W., Hirata, M., Balint, R. F., Lee, J., Zhong, J., and Wright, S. C. (1995) *Infect. Immun. 63*, 1291.
21. Levy, O., Ooi, C. E., Elsbach, P., Doerfler, M. E., Lehrer, R. I., and Weiss, J. (1995) *J. Immunol. 154*, 5403−5410.
22. Scott, M. G., Rosenberger, C. M., Gold, M. R., Finlay, B. B., and Hancock, R. E. (2000) *J. Immunol. 165*, 3358−3365.
23. Scott, M. G., Vreugdenhil, A. C., Buurman, W. A., Hancock, R. E., and Gold, M. R. (2000) *J. Immunol. 164*, 549−553.
24. Boman, H. G. (1995) *Annu. Rev. Immunol. 13*, 61−92.
25. Nicolas, P., and Mor, A. (1995) *Annu. Rev. Microbiol. 49*, 277−304.
26. Zasloff, M. (1992) *Curr. Opin. Immunol. 4*, 3−7.
27. Lehrer, R. I., and Ganz, T. (1999) *Curr. Opin. Immunol. 11*, 23−27.
28. Weersink, A. J., van Kessel, K. P., van den Tol, M. E., van Strijp, J. A., Torensma, R., Verhoef, J., Elsbach, P., and Weiss, J. (1993) *J. Immunol. 150*, 253−263.
29. Abrahamson, S. L., Wu, H. M., Williams, R. E., Der, K., Ottah, N., Little, R., Gazzano-Santoro, H., Theofan, G., Bauer, R., Leigh, S., Orme, A., Horwitz, A. H., Carroll, S. F., and Dedrick, R. L. (1997) *J. Biol. Chem. 272*, 2149−2155.
30. Lamping, N., Hoess, A., Yu, B., Park, T. C., Kirschning, C. J., Pfeil, D., Reuter, D., Wright, S. D., Herrmann, F., and Schumann, R. R. (1996) *J. Immunol. 157*, 4648−4656.
31. Juan, T. S., Hailman, E., Kelley, M. J., Wright, S. D., and Lichenstein, H. S. (1995) *J. Biol. Chem. 270*, 17237−17242.
32. Tam, J. P., Lu, Y.-A., and Yang J.-L. (2000) *Biochem. Biophys. Res. Commun. 267*, 783−790.
33. Tam, J. P., Wu, C., and Yang, J.-L. (2000) *Eur. J. Biochem. 267*, 3289−3300.
34. Tam J. P., Lu, Y.-A., and Yang, J.-L. (2000) *Biochemistry 39*, 7159−7169.
35. Tang, Y.-Q., Yuan, J., Ösapay, G., Ösapay, K., Tran, D., Miller, C. J., Ouellette, A. J., and Selsted, M. E. (1999) *Science 286*, 498−502.
36. Kokryakov, V. N., Harwig, S. S. L., Panyutich, E. A., Shevchenko, A. A., Aleshina, G. M., Shamova, O. V., Korneva, H. A., and Lehrer, R. (1993) *FEBS Lett. 327*, 231−236.
37. Nakamura, T., Furanaka, H., Miyata, T., Tokunaga, F., Muta, T., Iwanaga, S., Niwa, M., Taokao, T., and Shimonishi, Y. (1988) *J. Biol. Chem. 263*, 16709−16713.

38. Merrifield, R. B. (1963) *J. Am. Chem. Soc. 85*, 2149−2154.
39. Barany, G., and Merrifield, R. B. (1980) in *The Peptides 2* (Gross, E., and Meienhofer, J., Eds.) pp 1−284, Academic Press, New York.
40. Hojo, H., and Aimoto, S. (1991) *Bull. Chem. Soc. Jpn. 64*, 111−117.
41. Zhang, L., and Tam, J. P. (1997) *J. Am. Chem. Soc. 119*, 2363−2370.
42. Tam, J. P., and Lu, Y.-A. (1998) *Protein Sci. 7*, 1583−1592.
43. Zhang, L., and Tam, J. P. (1999) *J. Am. Chem. Soc. 121*, 3311−3320.
44. Wuthrich, K. (1986) in *NMR of Proteins and Nucleic Acids*, Wiley-Interscience, New York.
45. Woody, R. W. (1995) *Methods Enzymol. 246*, 34−71.
46. Lehrer, R. I., Rosenman, M., Harwing, S. S., Jackson, R., and Eisenhauer, P. (1991) *J. Immunol. Methods 137*, 167−173.
47. Ried, C., Wahl, C., Miethke, T., Wellnhofer, G., Landgraf, C., Schneider-Mergener, J., and Hoess, A (1996) *J. Biol. Chem. 271*, 28120−28127.
48. Breukink, E., Wiedemann, I., Kraaij, O. P., Kuipers, O. P., Sahl, H.-G., and de Kruijff, B., (1999) *Science 286*, 2361−2364.
49. Castle, M., Narzarian, A., Yi, S.-S., and Tempst, P. (1999) *J. Biol. Chem. 274*, 32555−32564.
50. Hoffmann, R., Bulet, P., Urge, L., and Otvos, L., Jr. (1999) *Biochim. Biophys. Acta 1426*, 459−467.
51. Gran, L. (1972) *Medd. Nor. Farm. Selsk. 34*, 125−135.
52. Tam, J. P., Lu, Y.-A., Yang, J.-L., and Chiu, K.-W. (1999) *Proc. Natl. Acad. Sci. U.S.A. 96*, 8913−8918.
53. IUPAC−IUB (1989) *J. Biol. Chem. 264*, 668−673.

BI0100384